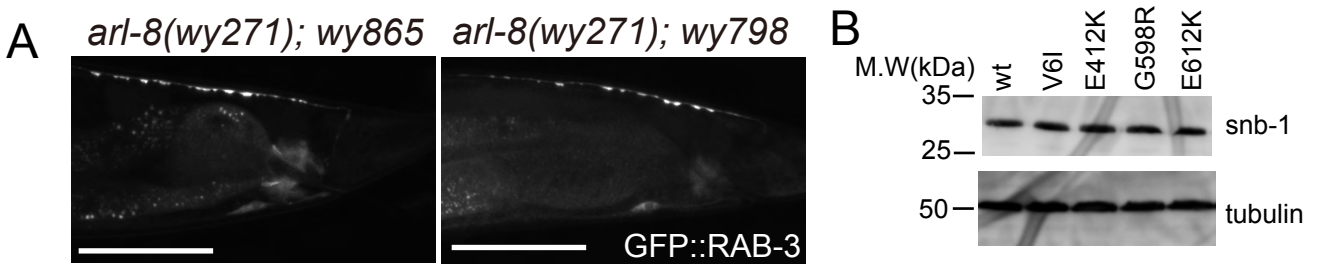

Niwa et al. Figure S1 (related to Figure 1)

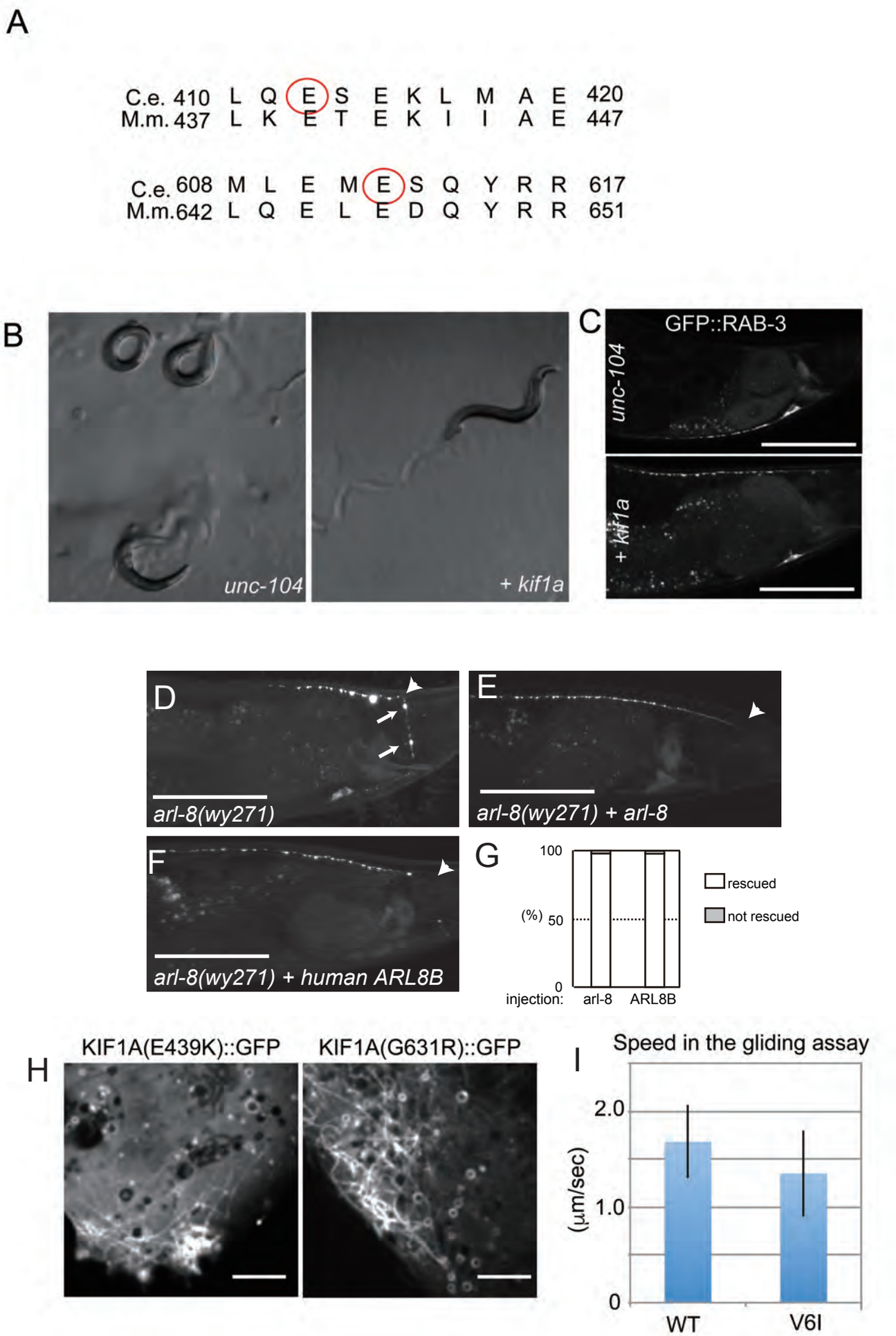

Niwa et al., Supplementary Figure S2 (related to Figure 2)

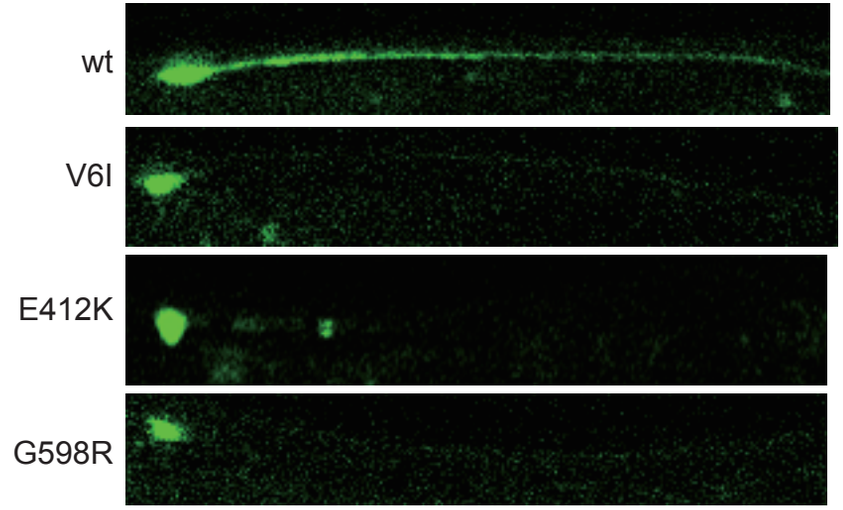

Niwa et al., Supplemental Figure S3

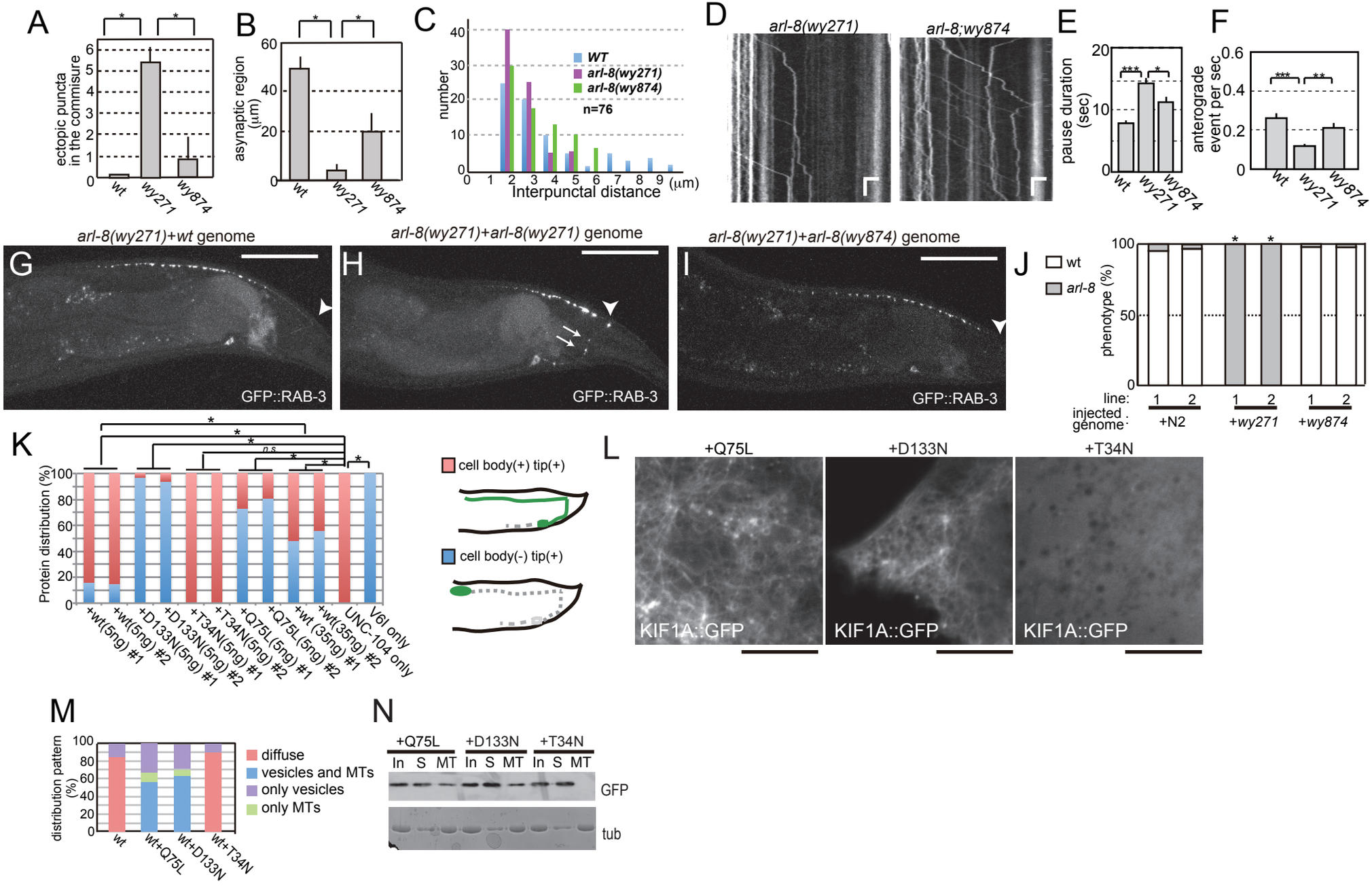

Niwa et al., Supplementary Figure S4 (related to Figure 6)

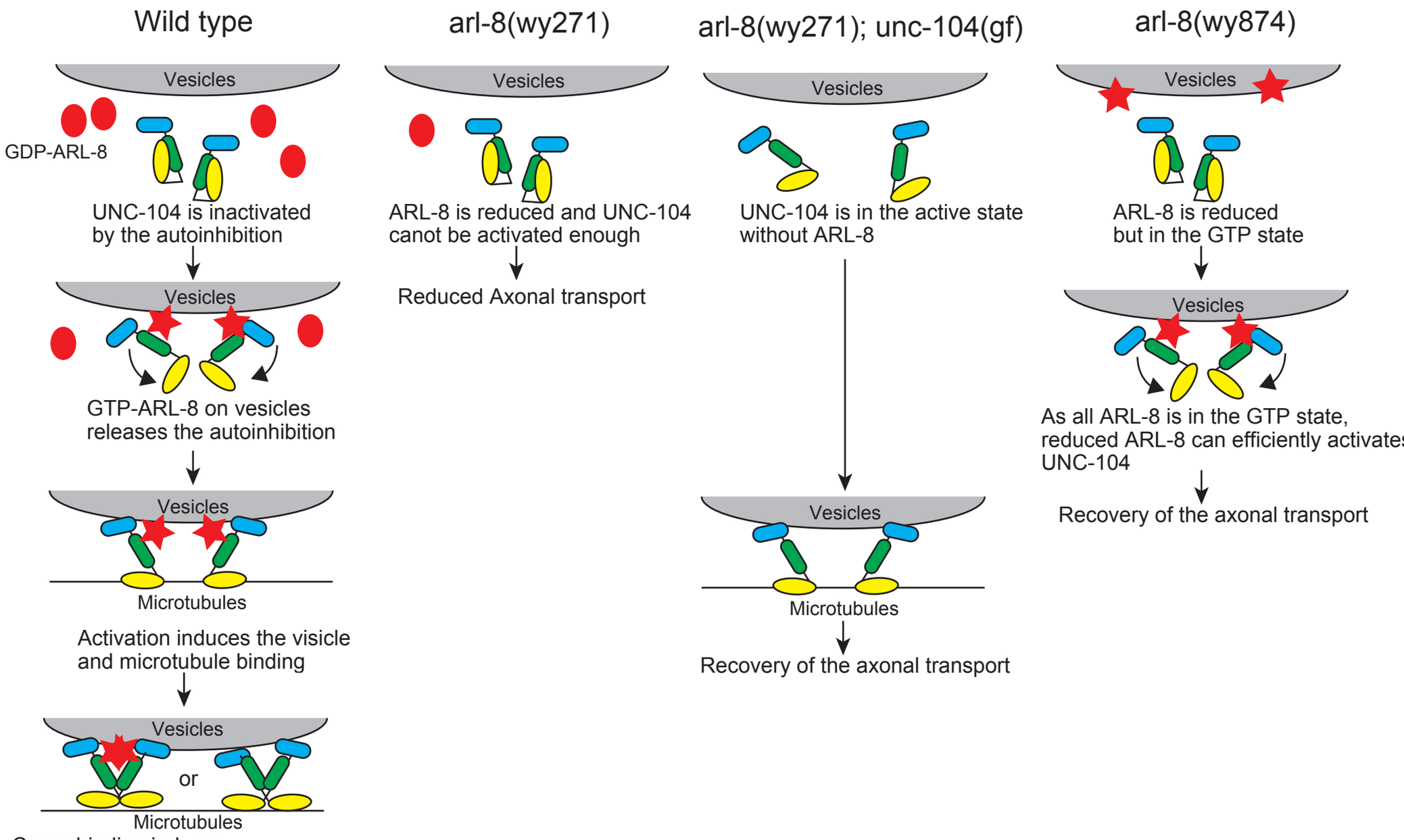

Niwa et al. Supplementary Figure S5

Supplementary Figure legends

Figure S1 (related to Figure 1)

(A) The representative images of unc-104(wy865) (V6I) and unc-104(wy798) (E412K). Bars, 50 μm

(B) A representative Western blotting showing the expression level of SNB-1. The amount of SNB-1 is not changed in unc-104(gf) alleles.

Figure S2 (related to Figure 2)

(A) The alignment of CC1 and CC2 mutations in Caenorhabditis elegans (C.e.) and Mus musculus (M.m.).

(B and C) (B) Representative images of unc-104(e1265) and animals that were rescued by KIF1A. KIF1A was expressed by the *unc-104* promoter. (C) The localization of synaptic vesicles in DA9 neurons. Bars, 50 μm.

(D-G) *arl-8(wy271)* is rescued by expressing arl-8 or human ARL8B. (D-F) Representative images showing (D) *arl-8(wy271)*, (E) *arl-8(wy271)* expressing *C. elegans arl-8*, and (F) *arl-8(wy271)* expressing human *ARL8B*. Bars, 50 μm. Pitr-1::arl-8 or Pitr-1::ARL8B were injected to arl-8(wy271) animals. Podr-1::GFP was used as a co-injection marker. Bars, 50 μm. (G) The synaptic vesicle phenotype was sorted as "rescued" or "not rescued". Note that both *arl-8* and human *ARL8B* could rescue the mislocalization of synaptic vesicles in the *arl-8* mutant.

(H) The localization of KIF1A(E439K)::GFP and KIF1A(G631R)::GFP in COS-7 cells. Bars, 5 μm.

(I) The motor domain of UNC-104 and UNC-104(V6I) were purified from E.coli using metal ion affinity chromatography. The speed of microtubules in microtubule gliding assays, n = 25. Mean ± Standard deviation.

Figure S3 (related to Figure 3)

Confocal images of the localization of UNC-104 and UNC-104 mutants visulalized by fusing with GFP. While wt UNC-104 is diffuse, UNC-104 mutants strongly accumulate to the tip of the DA9 axon and under the detectable level in the axonal shaft.

Figure S4 (related to Figure 6)

(A-C) Analysis of the distribution of GFP::RAB-3 positive puncta. (A and B) The

number of misaccumulation to the commissure region (A) and the distance of dorsal asynaptic region (B) were counted as Figure 1H. (C) The distribution of the interpunctal distance in wild type (WT), *arl-8(wy271)* and *arl-8(wy874)*. In *arl-8(wy874)*, the length of intersynapses is significantly longer compared to *arl-8(wy271)*. ($p < 0.01$, Mann–Whitney *U* test , n = 76 intersynapses from 4 animals), but is significantly shorter than wt ($p < 0.01$, Mann–Whitney *U* test , n = 76 intersynapses from 4 animals).

(D-F) Vesicle movement was analyzed as described in Figure 5. (D) Representative kymographs from *arl-8(wy271)* and *arl-8(wy874)*. Scale bars, 6 sec and 5 μm, respectively. Anterograde events have negative slope, and retrograde events have positive slope, from left to right. (E and F) Mean pause times per pause (E) and Anterograde frequency (F) in each genotype. Kruskal-Wallis test *, $p < 0.1$, **, $p < 0.05$ and ***, $P < 0.01$, respectively.

(G-J) Rescue of *arl-8(wy271)* by different genomic fragments. Genomic DNA amplified from indicated genotypes were injected into *arl-8(wy271)* animals. Representative images of animals that carry (G) wt genomic DNA, (H) *arl-8(wy271)* genomic DNA and (I) *arl-8(wy874)* genomic DNA. (J) Transgenic animals from two independent transgenic lines were scored for rescue and plotted. *, $p < 0.01$, compared to wt genomic injection, Chi-square test, n = 50 worms. Scale Bars, 50 μm.

(K) Subcellular localization of UNC-104(WT)::GFP in the presence of wt and mutant forms of ARL-8 mutants. As a control, the result of UNC-104(V6I) is shown as well. *, $p < 0.05$, Chi-square test with Bonferroni correction, n = 100 worms.

(L and M) ARL8B(Q75L), ARL8B(D133N) and ARL8B(T34N) were coexpressed with KIF1A::GFP and GFP signals were detected. Confocal images (L) and Statistical analysis (M). While The GDP mutant (T34N) did not activate KIF1A, the GTP mutants (Q75L and D133N) strongly drive KIF1A onto microtubules and vesicles. n = 30 cell, *, $p < 0..05$, Chi-square test with Bonferroni correction. Bars, 10 μm.

(N) Microtubule binding assay. KIF1A and ARL8B mutants were co-transfected to COS cells and microtubule binding assay was performed as described in Figure 2F. Note that the GTP mutants drive KIF1A to microtubule fraction.

Figure S5 (related to Figure 7)

In wild type, UNC-104 is in the inactive state by autoinhibition. GTP-ARL-8 on

synaptic vesicle precursors unlocks the autoinhibition of UNC-104. Activated UNC-104 can binds to both vesicles and microtubules.

In *arl-8(wy271)*, because of the promoter mutation (Fig. 7A), the amount of ARL-8 is not enough to activate UNC-104. This causes the reduction of axonal transport.

In *arl-8(wy271); unc-104(gf)*, UNC-104 is in the active state. Thus, axonal transport is sufficiently activated although the amount of ARL-8 is reduced.

In *arl-8(wy874)*, all the ARL-8 is in the GTP state. Then, UNC-104 can be sufficiently activated although the expression level of ARL-8 is reduced.

Supplemental Experimental Procedure

Worm genetics

C. elegans was maintained on OP50 feeder as described in the standard protocol (Brenner, 1974). Strains were maintained 20 °C and observed at room temperature except where otherwise noted.

Strains

wyIs85 [*Pitr-1::gfp::rab-3, Podr-1::dsred*], *arl-8(wy271)*; *wyIs85* and *unc-104(wy673)* were described previously (Klassen and Shen, 2007; Klassen et al., 2010; Wu et al., 2013).

Genetic modifier screens of arl-8 mutant

arl-8(*wy271*); *wyIs85* L4 animals were treated with EMS as described (Wu et al., 2013). Worms were maintained at 20 °C. F1 self progenies were screen under a 63X objective on an AxioPlan2 upright microscope for GFP::RAB-3 distribution phenotypes that deviate from that of the starting strain.

Antibodies and plasmids

unc-104 cDNA was amplified by PCR and cloned into pSM GFP vector (a gracious gift of Steven McCarroll and Cori Bargmann). Then the *itr-1* promoter is ligated to the upstream of *unc-104* cDNA. The KIF1A::GFP vector and the anti-KIF1A antibody are described previously (Niwa et al., 2008). Anti-GFP antibody (#598) was obtained from MBL (Nagoya, Japan). TUBB5::TagRFP is described previously (Niwa et al., 2013). Anti-snb-1 antibody was described previously (Hadwiger et al., 2010).

To introduce gain-of-function mutations into *unc-104* and KIF1A vectors, PCR based mutagenesis was performed using KOD-plus-high fidelity DNA polymerase (TOYOBO, Tokyo, Japan).

Microtubule binding assay

293T cells (Life Technologies, Waltham, MA, USA) were maintained in DMEM medium (Life Technologies) supplemented with 10% FBS (Life Technologies) in a CO2 incubator at 37 °C. One day before the transfection, cells were transferred to ⌀10 cm dishes. Vectors encoding KIF1A::GFP and its mutants were transfected by Lipofectamine 2000 (Life Technologies) as described in the manufacture's protocol and incubated for 36 hours. Cells were lysed in PEM buffer (100 mM Pipes, 1mM EGTA and 1mM $MgCl_2$) supplemented with 0.1 % Triton-X100 and a complete mini proteinase inhibitor tablet (Roche, Basel, Swiss). Debris was removed by ultracentrifuge using a TLA-55 rotor (Beckman Coulter, Brea, CA, USA) at 45,000 rpm at 4 °C for 10 min. Lysate fractions were used as input fractions (In). 10 μM tubulin purified from porcine brains and 0.5 mM AMP-PNP were added and incubated for 10 min at

37 °C. Then, 20 μM taxol was added and incubated for another 10 min at 37 °C. Polymerized microtubules (MT) and supernatant (S) fractions were separated by ultracentrifuge at 45000 rpm 27 °C for 10 min. Each fraction was analyzed by western blot using the anti-GFP antibody.

GST pull down

GST-fused ARL8B and ARL-8 mutants were expressed in BL21RIL (Agilent Technologies, Santa Clara, CA, USA). Cells transformed with GST, GST-ARL8B, GST-ARL8B(T34N) and GST-ARL8B(Q75L) vectors were cultured in 5 ml LB medium supplemented with 50 mg/ml ampicillin. Cells with the GST-ARL8B(D133N) vector were cultured in 30 ml medium due to low expression level . Protein expression was induced by 0.2 mM Isopropyl β-D-1-thiogalactopyranoside (IPTG) and cultured for 16 hours at 18 °C. Cells were collected by a bench top centrifuge (Beckman) at 3000 g for 10 min at room temperature and then lysed in B-PER reagent (Thermo Scientific, Waltham, MA, USA) at 4 °C. Lysate was separated by centrifuge at 15000 rpm for 10 min at 4 °C. Into the lysate, 40 ul bed volume of Glutathione sepharose 4B (GE Healthcare Life Science, Pittsburgh, PA, USA) was added and incubated for 1 hour. After the incubation, beads were washed twice with immunoprecipitation buffer (10 mM Tris, pH 7.4, 150 mM NaCl, 0.1 % Nonidet P40). Proteins were eluted by SDS-PAGE sample buffer (125 mM Tris, pH 6.8, 4 % SDS, 20 % Glycerol, 0.01 % bromophenol blue) freshly supplemented with 10 % volume of 2-mercaptoethanol (Sigma Aldrich) and boiled at 95 °C.

C. elegans transgenesis

Injection was performed as described (Mello and Fire, 1995). Glass needles were prepared using a MODEL P-2000 micropipette puller (Sutter Instrument, Novato, CA, USA). A FemtoJet microinjection system (Eppendorf, Hamburg, Germany) was used for microinjection.

Confocal microscopy

wyIs85 [Pitr-1::gfp::rab-3; Podr-1::rfp] was used as a synaptic vesicle marker in DA9 neuron. Animals were fixed by 4 % Paraformaldehyde on the 5% agarose pad prepared as described. Images were taken using an Axio Observer. Z1 microscope equipped with a LSM710 confocal system (Carl Zeiss) using Plan-Apochromat (x63, N.A. 1.4) objective lens. Z stack images were saved as the lsm format, analyzed and reconstituted using NIH image.

Computer-based Image analysis

Computer-based image analysis was performed as described (Crane et al., 2012). In short, *C. elegans*

individuals are suspended in fluid, that pressure driven into the imaging chamber of a polydimethylsiloxane (PDMS) soft microfluidic device. Pneumatic, automatically-controlled valves temporarily confine individuals for epifluorescent imaging, discarding individuals that do not display DA9 in the imaging region. A previously-trained support vector machine (SVM) algorithm is used to identify synapses within the images obtained, and custom software extracts synaptic properties from the synapses identified (Chung et al., 2008; Crane et al., 2010).

Live cell imaging

Axonal transport was visualized using *wyIs251 [Pmig-13::gfp::rab-3; Pord-1::gfp]* as described. Worms were anesthetized in M9 buffer supplemented with 2 mM Levamisole and mounted on 5% agarose pad on a slide. Time-lapse imaging was performed on a spinning disk confocal microscope with a Plan-Apochromat 100x/1.4 objective and a 1.6x intermediate lens. Images were taken at 4 flames per second for 1 min. Movies were analyzed by NIH image.

arl-8 rescue

The *arl-8* genomic fragments were amplified by polymerase chain reaction (PCR) using 5'-TAAGCGGCGAGAACCGACATGCGTG-3' and 5'-CGCCTTCAAGAAATACAGTACCCCAC-3'. KOD-plus-DNA polymerase kit (TOYOBO, Tokyo, Japan) was used with a slight modification. For efficient reaction, 0.5 μl of Taq DNA polymerase (New England Biolabs, USA) was added to each 50 μl reactions.

Microtubule gliding assays

Microtubule gliding assay was performed as described (Carter and Cross, 2001; Niwa et al., 2012). The vector encoding the motor domain of UNC-104 was obtained from Addgene (Pierce et al., 1999). Proteins were expressed in BL21RIL(DE3) and purified by TALON Ni^{2+} sepharose (Takara-Clontech, Tokyo, Japan). The gliding assay was performed in the flow chamber, consisting of 24- x 40 -mm and 18- x 18-mm glass coverslips (Matsunami, Tokyo, Japan), attached by double-sided tape (3M, Maplewood, MN, USA). Purified motors were diluted in gliding assay buffer (80 mM Pipes, pH 6.9, 1mM EGTA, 1mM $MgCl_2$, 1 mM DTT, 10 mM taxol, 0.5 mg/ml casein) and fixed on the coverslip using anti-penta-His antibody (Qiagen). TMR-labeled microtubules were flowed. ELYRA P.1 system (Carl Zeiss) was used in the total internal fluorescent microscopy (TIRF) mode.

Visualization of KIF1A and microtubule in COS-7 cells

Compared to unfixed cells (Figure 2B), KIF1A-GFP was detached in cells fixed by the 4% paraformaldehyde or cold methanol. Thus, we coexpressed TUBB5-TagRFP in order to visualize microtubules as described (Niwa et al., 2013). Cells were directly observed by spinning disc microscopy as described above.

Statistics

Statistical methods and the sample size are described in each figure legends. t-test and Chi-square tests and Bonferroni correction were performed using Excel (Microsoft Corporation, Redmond, WA, USA), Mann–Whitney *U* test was performed using Excel Toukei (SSRI, Tokyo, Japan) and Kruskal-Wallis test was performed using MATLAB (MathWorks, Natick, MA, USA).

Supplementary References

Brenner, S. (1974). The genetics of Caenorhabditis elegans. Genetics 77, 71-94.

Carter, N., and Cross, R. (2001). An improved microscope for bead and surface-based motility assays. Methods Mol Biol 164, 73-89.

Chung, K., Crane, M.M., and Lu, H. (2008). Automated on-chip rapid microscopy, phenotyping and sorting of C. elegans. Nat Methods 5, 637-643.

Crane, M.M., Chung, K., Stirman, J., and Lu, H. (2010). Microfluidics-enabled phenotyping, imaging, and screening of multicellular organisms. Lab Chip 10, 1509-1517.

Crane, M.M., Stirman, J.N., Ou, C.Y., Kurshan, P.T., Rehg, J.M., Shen, K., and Lu, H. (2012). Autonomous screening of C. elegans identifies genes implicated in synaptogenesis. Nat Methods 9, 977-980.

Hadwiger, G., Dour, S., Arur, S., Fox, P., and Nonet, M.L. (2010). A monoclonal antibody toolkit for C. elegans. PLoS One 5, e10161.

Klassen, M.P., and Shen, K. (2007). Wnt signaling positions neuromuscular connectivity by inhibiting synapse formation in C. elegans. Cell 130, 704-716.

Klassen, M.P., Wu, Y.E., Maeder, C.I., Nakae, I., Cueva, J.G., Lehrman, E.K., Tada, M., Gengyo-Ando, K., Wang, G.J., Goodman, M.*, et al.* (2010). An Arf-like small G protein, ARL-8, promotes the axonal transport of presynaptic cargoes by suppressing vesicle aggregation. Neuron 66, 710-723.

Mello, C., and Fire, A. (1995). DNA transformation. Methods Cell Biol 48, 451-482.

Niwa, S., Nakajima, K., Miki, H., Minato, Y., Wang, D., and Hirokawa, N. (2012). KIF19A is a microtubule-depolymerizing kinesin for ciliary length control. Dev Cell 23, 1167-1175.

Niwa, S., Takahashi, H., and Hirokawa, N. (2013). β-Tubulin mutations that cause severe neuropathies disrupt axonal transport. EMBO J 32, 1352-1364.

Niwa, S., Tanaka, Y., and Hirokawa, N. (2008). KIF1Bbeta- and KIF1A-mediated axonal transport of presynaptic regulator Rab3 occurs in a GTP-dependent manner through DENN/MADD. Nat Cell Biol 10, 1269-1279.

Pierce, D.W., Hom-Booher, N., Otsuka, A.J., and Vale, R.D. (1999). Single-molecule behavior of monomeric and heteromeric kinesins. Biochemistry 38, 5412-5421.

Wu, Y.E., Huo, L., Maeder, C.I., Feng, W., and Shen, K. (2013). The balance between capture and dissociation of presynaptic proteins controls the spatial distribution of synapses. Neuron 78, 994-1011.